JOURNAL OF MATERIALS SCIENCE 33 (1998) 2027–2037

Electric modulus and interfacial polarization in composite polymeric systems

G. M. TSANGARIS*, G. C. PSARRAS, N. KOULOUMBI
Chemical Engineering Department, Materials Science and Engineering Section, National Technical University, 9, Iroon Polytechniou Street, Athens 157 80, Greece
E-mail: gtsang@orfeas.chemeng.ntua.gr

The applicability of the electric modulus formalism is investigated on a Debye-type relaxation process, the interfacial polarization or Maxwell–Wagner–Sillars effect. Electric modulus, which has been proposed for the description of systems with ionic conductivity and related relaxation processes, presents advantages in comparison to the classical approach of the real and imaginary part of dielectric permittivity. In composite polymeric materials, relaxation phenomena in the low-frequency region are attributed to the heterogeneity of the systems. For the investigation of these processes through electric modulus formalism, hybrid composite systems consisting of epoxy resin–metal powder–aramid fibres were prepared with various filler contents and their dielectric spectra were recorded in the frequency range 10 Hz–10 MHz in the temperature interval 30–150 °C. The Debye, Cole–Cole, Davidson–Cole and Havriliak–Negami equations of dielectric relaxation are expressed in the electric modulus form. Correlation between experimental data and the various expressions produced, shows that interfacial polarization in the systems examined is, mostly, better described by the Davidson–Cole approach and only in the system with the higher heterogeneity must the Havriliak–Negami approach be used.

1. Introduction

Interfacial polarization, termed the Maxwell–Wagner–Sillars (MWS) effect [1–3], is observed in heterogeneous systems composed of two or more phases. As a result of the difference in conductivities and permittivities of the constituents, space-charge build-up occurs at the macroscopic interfaces. The accumulation of charges changes the electric field, in contrast to the other types of polarization (atomic, electronic, dipolar) which are produced by the displacement or orientation of bound charge carriers.

A theoretical approach to the subject in terms of dielectric theory leads to a Debye-type relaxation [4]. Suitable dispersion equations describing the phenomenon are given by Van Beck [5], Von Hippel [6] and Böettcher and Bordewijk [7].

In polymers and composite polymeric materials, interfacial polarization is almost always present because of additives, fillers or even impurities which make these systems heterogeneous. Usually, in systems with a conductive component, interfacial relaxation is obscurred by conductivity and the dielectric permittivity may be as high as 1000 at low frequencies [8]. To overcome this difficulty in the study of interfacial polarization, it has been decided to use the formalism "electric modulus", first introduced by McCrum *et al.* [9]. Macedo *et al.* [10] were the first to exploit the modulus and used it for the investigation of electrical relexation phenomena in vitreous ionic conductors. It has also been used in polymers to study their conductivity relaxation behaviour [11–14].

Electrical relaxation phenomena are usually analysed in terms of the dielectric permittivity by the relaxation of the electric displacement vector, $\boldsymbol{D}$, under the constraint of constant electric field, $\boldsymbol{E}$. However, in dielectrics containing mobile charges, it seems convenient to concentrate on the relaxation of the electric field, $\boldsymbol{E}$, under the constraint of a constant displacement vector, $\boldsymbol{D}$ [15], which leads to the inverse dielectric permittivity and the definition of electric modulus. An advantage of using the electric modulus to interpret bulk relaxation properties is that variations in the large values of permittivity and conductivity at low frequencies are minimized. In this way the familiar difficulties of electrode nature and contact, space charge injection phenomena and absorbed impurity conduction effects, which appear to obscure relaxation in the permittivity presentation, can be resolved or even ignored [11].

Complex modulus, electric modulus or inverse complex permittivity, M^*, is defined by the following equation

$$M^* = \frac{1}{\varepsilon^*} = \frac{1}{\varepsilon' - j\varepsilon''} = \frac{\varepsilon'}{\varepsilon'^2 + \varepsilon''^2} + j\frac{\varepsilon''}{\varepsilon'^2 + \varepsilon''^2}$$
$$= M' + jM'', \qquad j = (-1)^{1/2} \tag{1}$$

*Author to whom all correspondence should be addressed.

where M' is the real and M'' the imaginary electric modulus, and ε' the real and ε'' the imaginary permittivity.

It is interesting to adapt the above formalism to study interfacial polarization in composite polymeric materials which have metal powder as one of their constituents.

In this work, hybrid polymeric composites [16], consisting of an epoxy resin matrix having, as fillers, Kevlar fibres and aluminium particles in various proporitons, were examined, using electric modulus. The original equations of dielectric dispersion with one relaxation time or distribution of relaxation times, either symmetric or asymmetric, are expressed in the electric modulus form and used accordingly.

2. Experimental procedure

A commercially available bisphenol-type epoxy resin (Epikote 828, Shell Co.) was used as a prepolymer having molecular weight ~ 320 and viscosity 25 000 mPa s at 25 °C. As curing agent, triethylene tetramine at 8 p.h.r. (parts of curing agent per hundred parts of resin) was employed. The product Kevlar 49 aramid pulp of E.I Du Pont de Nemours was used as filler which had the following properties: mean length of fibres 2 mm, diameter ~ 14 μm and density 1.44 g cm^{-3} [17]. Before use, it was dried at 100 °C for 2 h. Aluminium powder (Merck) was also used as filler which consisted of particles that were ellipsoidal in shape with varying size distribution, Fig. 1a, b.

Composites with 0, 0.5, 1.0, 1.5 p.h.r. in Kevlar fibres and aluminium powder 0, 5, 15, 25 p.h.r., were prepared. For every content of aluminium powder in the epoxy resin, four specimens were prepared with the above varying content of Kevlar fibres. The preparation was carried out as follows: epoxy prepolymer was heated at 60 °C, and then distilled acetone containing the required Kevlar pulp quantity was added to the resin. The mixture was heated to 130 °C to remove the acetone, then cooled freely to 60 °C and the curing agent was added. Afterwards the required quantity of aluminium powder was added with continuous stirring. The composite was then poured into suitable plexiglass moulds. Initial curing was carried out at ambient conditions for 24 h, followed by post-curing at 100 °C for 48 h.

Specimens in circular disc form, 60 mm diameter and 3 mm thick, were produced by machining the original castings. Satisfactorily homogeneous composites were produced, exhibiting no visible flaws or voids. The faces of the specimens were painted with silver paint to improve contact and were stored in a vacuum desiccator in the presence of silica gel for at least 5 d before measurement, to avoid any influence of moisture.

Dielectric measurements were performed using a video-bridge (T2100 of Electro Scientific Instruments Co.) in the frequency range 20 Hz–20 kHz and an impedance analyser (4192A Hewllet Packard) in the frequency range 20 kHz to 10 MHz. The test cell was a three-terminal guarded system according to ASTM D150-92 and D257-91 specifications. Details of the test cell are given elsewhere [18]. Measurements were performed in the temperature range 30–150 °C. D.c. conductivity measurements were performed using the conductivity cell HP 16008B and the high-resistance meter HP 4339A Hewlett Packard.

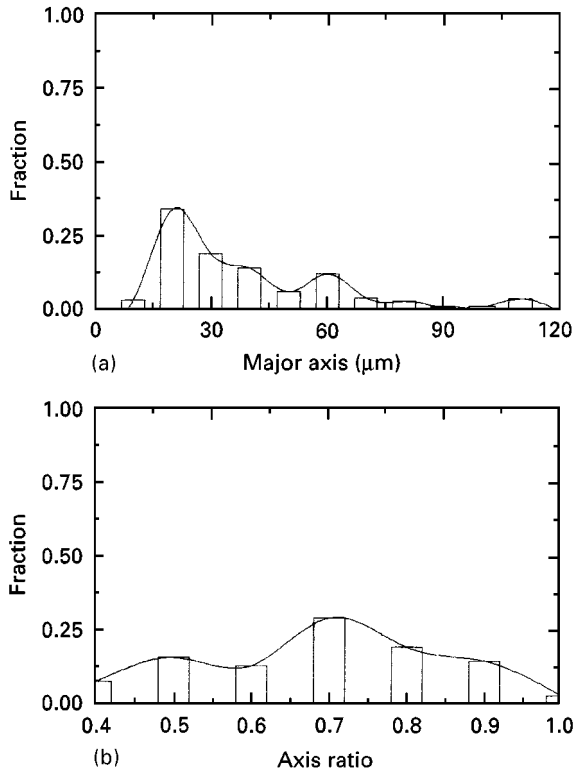

Figure 1 Particle-size distribution of aluminium powder: (a) major axis, (b) axis ratio.

3. Results

The change in the real, M', ε', and imaginary, (M'', ε''), parts of the electric modulus and dielectric permittivity versus frequency is shown in Figs 2 and 3 for two values of the content of Kevlar fibres and constant aluminium content at different temperatures. It can be clearly seen that values of (M') increase with frequency and reach a rather constant value, while values of ε', as expected, decrease to an almost constant value. In the frequency range of this transition, peaks in the values of M'', are developed, indicating a relaxation process which is not evident in the values of ε''. An increase in temperature leads to a decrease in the values of M', (increase in ε') in the low-frequency range, but is ineffective at higher frequencies (Figs 2a, b, 3a, b). Increasing the temperature shifts the peaks of M'' to higher frequencies, as shown in Figs 2c and 3c. Finally, increasing the content of Kevlar fibres decreases the values of M', but increases the peak values of M''.

In Fig. 4, the imaginary parts of electric modulus (a) and dielectric permittivity (b) versus frequency are shown for three different Kevlar fibre contents at the temperature of 150 °C. In the dielectric loss presentation, Fig. 4b, losses are high and do not form any peak in the frequency window of the measurements. In the electric modulus presentation, Fig. 4a, peaks are formed, their maxima increase with Kevlar content and

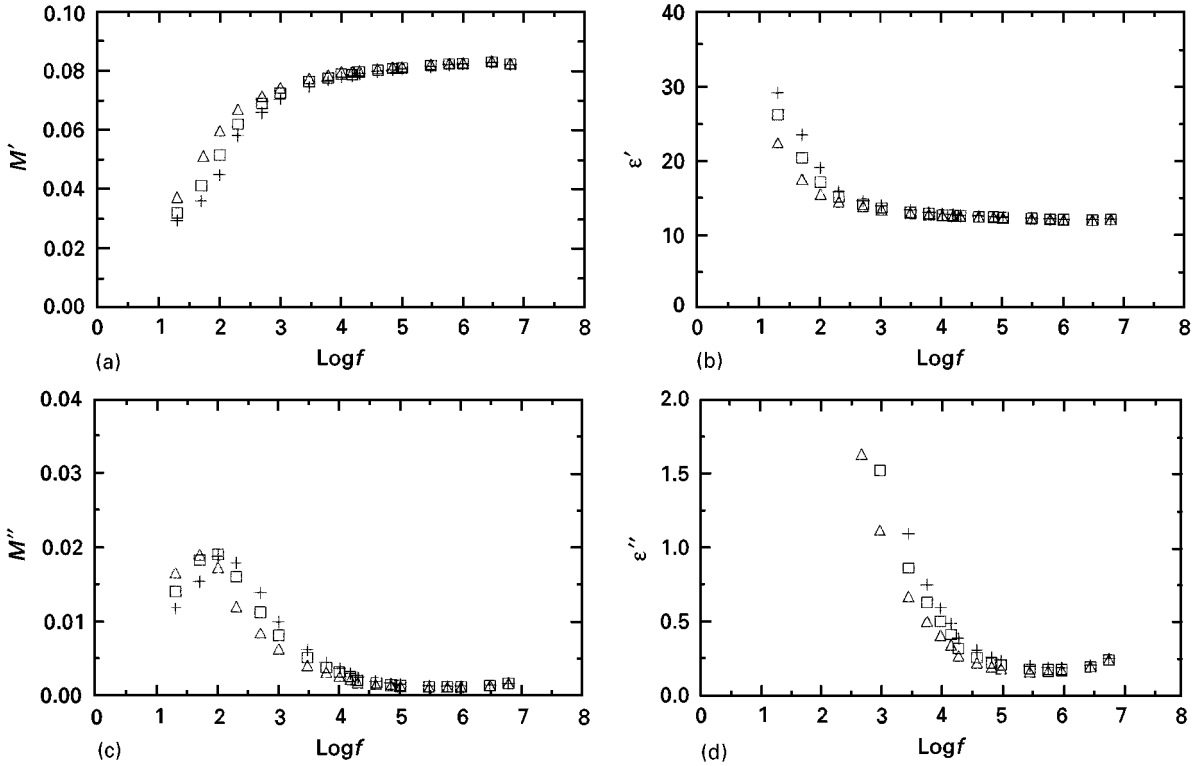

Figure 2 (a, b) Real M', ε' and (c, d) imaginary M'', ε'' parts of electric modulus and dielectric permittivity versus frequency for various temperatures of the composite with 25 p.h.r. in Al and 0.5 p.h.r. in Kevlar fibres. (△) 140 °C, (□) 145 °C, (+) 150 °C.

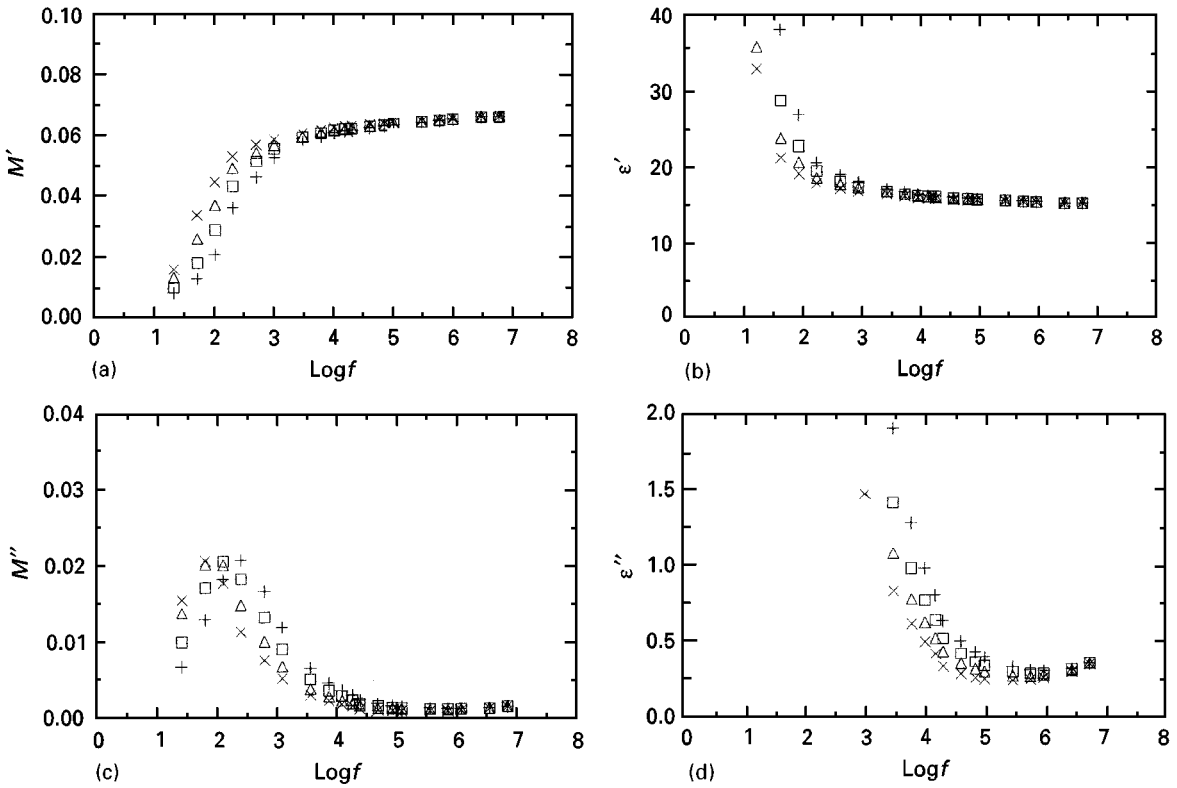

Figure 3 (a, b) Real M', ε' and (c, d) imaginary M'', ε'' parts of electric modulus and dielectric permittivity versus frequency for various temperatures of the composite with 25 p.h.r. in Al and 1.5 p.h.r. in Kevlar fibres. (×) 135 °C, (△) 140 °C, (□) 145 °C, (+) 150 °C.

shift slightly at the same time towards the left side of the frequency spectrum, thus providing means for study of relaxation.

The Cole–Cole graph for the electric moduli of the two systems depicted in Figs 2a, c and 3a, c, is shown in Fig. 5. In both cases, the graph resembles a suppressed semicircle implying a certain deviation from the pure Debye behaviour. Increasing the Kevlar content moves the semicircle towards the origin. This behaviour was shown by all specimens.

4. Discussion

The time dependence of the electric field, $\boldsymbol{E}$, and the displacement vector, $\boldsymbol{D}$, in a dielectric medium can be described by the differential equation [9]

$$\tau_{\boldsymbol{E}} \frac{\mathrm{d}\boldsymbol{D}(t)}{\mathrm{d}t} + \boldsymbol{D}(t) = \tau_{\mathrm{E}} \varepsilon_0 \varepsilon_\infty \frac{\mathrm{d}\boldsymbol{E}(t)}{\mathrm{d}t} + \varepsilon_0 \varepsilon_{\mathrm{S}} \boldsymbol{E}(t) \quad (2)$$

where $\tau_{\boldsymbol{E}}$ is the relaxation time under the constraint of constant electric field, and ε_{s}, ε_∞ are the limiting values of permittivity, when $\omega \to 0$ and $\omega \to \infty$, respectively. In the case of constant displacement vector and time-varying electric field, the solution of the above equation is

$$E(t) = \frac{D_0}{\varepsilon_0}\left[\left(\frac{1}{\varepsilon_\infty} - \frac{1}{\varepsilon_{\mathrm{s}}}\right) e^{-\frac{t}{\tau_{\boldsymbol{D}}}} + \frac{1}{\varepsilon_{\mathrm{s}}}\right] \quad (3)$$

where $\tau_{\boldsymbol{D}} = (\varepsilon_\infty/\varepsilon_{\mathrm{s}})/\tau_{\mathrm{E}}$ is the relaxation time under the constraint of constant displacement vector. Using the notation M_{S} for the value of M' when $\omega \to 0$ and M_∞ when $\omega \to \infty$, it is found from Equation 1 that

$$M_{\mathrm{s}} = \frac{1}{\varepsilon_{\mathrm{s}}} \quad (4a)$$

and

$$M_\infty = \frac{1}{\varepsilon_\infty} \quad (4b)$$

therefore the relationship between the time constants, in the modulus mode, becomes $\tau_{\mathrm{D}} = (M_{\mathrm{s}}/M_\infty)\,\tau_{\boldsymbol{E}}$. Because $M_{\mathrm{s}} < M_\infty$, then $\tau_{\boldsymbol{D}} < \tau_{\boldsymbol{E}}$ and a relation between the frequencies, where the peak losses occur in the two different modes, is obtained

$$f_{M,\,\max} = \frac{M_\infty}{M_{\mathrm{s}}} f_{\varepsilon,\,\max} \quad (5)$$

$f_{M,\,\max}$ and $f_{\varepsilon,\,\max}$ are the frequencies where the maximum losses are occurring in the modulus and permittivity mode.

Considering the influence, on a dielectric system, of a frequency-dependent electric field, $\boldsymbol{E}$, and displacement vector, $\boldsymbol{D}$, and using the relation

$$M^* = \frac{1}{\varepsilon^*} = \frac{\boldsymbol{E}(\omega)}{\varepsilon_0 \boldsymbol{D}(\omega)} \quad (6)$$

the solution of Equation 2 can be written

$$M^* = \frac{1}{\varepsilon^*} = \frac{\boldsymbol{E}(\omega)}{\varepsilon_0 \boldsymbol{D}(\omega)} = M_{\mathrm{s}} M_\infty \frac{1 + j\omega\tau}{M_\infty + M_{\mathrm{s}}(j\omega\tau)} \quad (7)$$

Resolving the real and imaginary part of Equation 7, Equations 8 and 9 are produced, which describe the electric field relaxation, in the frequency domain mode for a single relaxation time, in terms of electric modulus

$$M' = M_\infty M_{\mathrm{s}} \frac{M_\infty + M_{\mathrm{s}}\omega^2\tau^2}{M_\infty^2 + M_{\mathrm{s}}^2\omega^2\tau^2} \quad (8)$$

$$M'' = M_\infty M_{\mathrm{s}} \frac{(M_\infty - M_{\mathrm{s}})\omega\tau}{M_\infty^2 + M_{\mathrm{s}}^2\omega^2\tau^2} \quad (9)$$

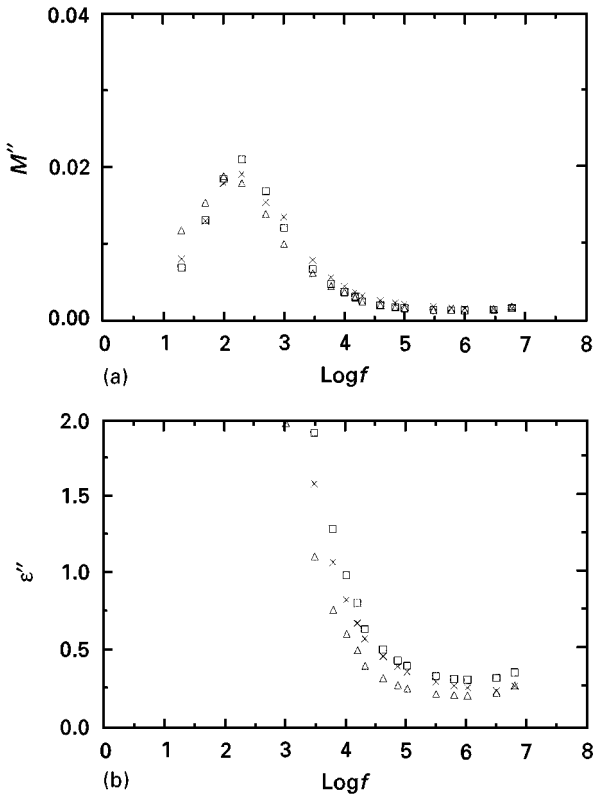

Figure 4 Imaginary parts of (a) electric modulus and (b) dielectric permittivity of composites with varying Kevlar content, at the temperature of 150 °C. Al 25 p.h.r. and Kevlar (△) 0.5 p.h.r., (×) 1.0 p.h.r., (□) 1.5 p.h.r.

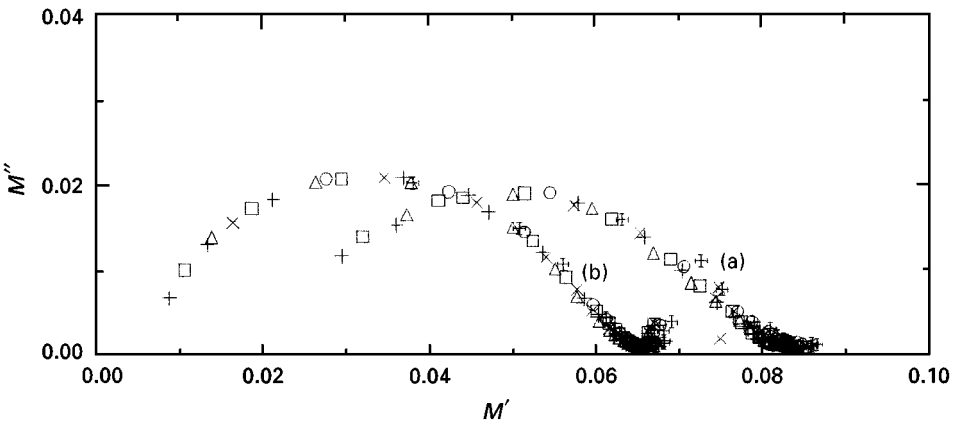

Figure 5 Cole–Cole plots of the hybrid composites with 25 p.h.r. in Al and (a) 0.5 p.h.r., (b) 1.5 p.h.r. in Kevlar fibres. (+) 125 °C, (○) 130 °C, (×) 135 °C, (△) 140 °C, (□) 145 °C, (+) 150 °C.

The above equations are equivalent with the very well-known Debye's dispersion equations.

Elimination of ωt between Equations 8 and 9 leads to the equation

$$\left(M' - \frac{M_\infty + M_s}{2}\right)^2 + M''^2 = \left(\frac{M_\infty - M_s}{2}\right)^2 \quad (10)$$

which represents a semicircle with radius $r = (M_\infty - M_s)/2$ and centred at a distance $(M_\infty + M_s)/2$ from the origin, in complete accordance with the corresponding equation in Debye's treatment.

The influence of the distribution of relaxation times, in the permittivity mode, has been introduced by Cole–Cole [19–21]. In order to include the influence of the distribution of relaxation times in Equations 8 and 9, the Cole–Cole equations are combined with Equation 1 and the expressions below are derived

$$M' = M_\infty M_s \times \frac{[M_s A + (M_\infty - M_s)\cos\phi]\,A}{M_s^2 A^2 + 2A(M_\infty - M_s)M_s\cos\phi + (M_\infty - M_s)^2} \quad (11)$$

$$M'' = M_\infty M_s \times \frac{[(M_\infty - M_s)\sin\phi]\,A}{M_s^2 A^2 + 2A(M_\infty - M_s)M_s\cos\phi + (M_\infty - M_s)^2} \quad (12)$$

Here

$$A = \left[1 + 2(\omega\tau)^{1-\alpha}\sin\frac{\pi\alpha}{2} + (\omega\tau)^{2(1-\alpha)}\right]^{1/2} \quad (13)$$

and

$$\phi = \alpha\,\mathrm{rc\,tg}\left[(\omega\tau)^{1-\alpha}\cos\frac{\alpha\pi}{2}\Big/1 + (\omega\tau)^{(1-\alpha)}\sin\frac{\alpha\pi}{2}\right] \quad (14)$$

It can be seen that for $\alpha = 0$ the above expressions reduce to Equations 8 and 9 for a single relaxation time.

From Equations 11 and 12 the following expression representing the equation of a semi-circle can be derived

$$\left[M' - \frac{1}{2}(M_\infty + M_s)\right]^2 + \left[M'' + \frac{1}{2}(M_\infty - M_s)\,\mathrm{tg}\frac{\alpha\pi}{2}\right]^2 = \left[\frac{1}{2}(M_\infty - M_s)\sec\frac{\alpha\pi}{2}\right]^2 \quad (15)$$

The radius of the semicircle is $r = \frac{1}{2}(M_\infty - M_s)\sec(\alpha\pi/2)$ and the centre lies below the x-axis, having co-ordinates $\frac{1}{2}(M_\infty + M_s)$ and $-\frac{1}{2}\times(M_\infty - M_s)\,\mathrm{tg}\,(\alpha\pi/2)$.

Davidson and Cole [22], aiming to account for an asymmetric distribution of relaxation times resulting from a dielectric dispersion within a system, introduced the parameter γ in Debye's dielectric function.

Using the same procedure, as in the Cole–Cole consideration, the Davidson–Cole equations are changed into the electric modulus form and have the expressions

$$M' = \frac{M_\infty M_s[M_s + (M_\infty - M_s)(\cos\phi)^\gamma\cos\gamma\phi]}{M_s^2 + (M_\infty - M_s)(\cos\phi)^\gamma[2M_s\cos\gamma\phi + (M_\infty - M_s)(\cos\phi)^\gamma]} \quad (16)$$

$$M'' = \frac{M_\infty M_s(M_\infty - M_s)(\cos\phi)^\gamma\sin\gamma\phi]}{M_s^2 + (M_\infty - M_s)(\cos\phi)^\gamma[2M_s\cos\gamma\phi + (M_\infty - M_s)(\cos\phi)^\gamma]} \quad (17)$$

where

$$0 < \gamma \le 1 \quad (18a)$$

$$\mathrm{tg}\,\phi = \omega\tau \quad (18b)$$

$$\omega_{max}\tau = \mathrm{tg}\left(\frac{1}{\gamma+1}\frac{\pi}{2}\right) \quad (18c)$$

Equations 16 and 17 for $\gamma = 1$ are reduced to the corresponding Equations 8 and 9 for a pure Debye process.

The generalization introduced by Havriliak and Negami [23], in the permittivity mode, can also be expressed in terms of M' and M'' as follows

$$M' = M_\infty M_s \times \frac{[M_s A^\gamma + (M_\infty - M_s)\cos\gamma\phi]\,A^\gamma}{M_s^2 A^{2\gamma} + 2A^\gamma(M_\infty - M_s)M_s\cos\gamma\phi + (M_\infty - M_s)^2} \quad (19)$$

$$M'' = M_\infty M_s \times \frac{[(M_\infty - M_s)\sin\gamma\phi]\,A^\gamma}{M_s^2 A^{2\gamma} + 2A^\gamma(M_\infty - M_s)M_s\cos\gamma\phi + (M_\infty - M_s)^2} \quad (20)$$

where A and ϕ are given by Equations 13 and 14. Equations 19 and 20 give:

for $\gamma = 1$ and $\alpha = 0$ the Debye Equations 8, 9
for $\gamma = 1$ and $\alpha \neq 0$ the Cole–Cole Equations 11 and 12, and
for $\gamma \neq 1$ and $\alpha = 0$ the Davidson–Cole Equations 16, and 17.

In the case of a heterogeneous material, the dispersion equation describing interfacial polarization [3] is

$$\varepsilon^* = \varepsilon'_\infty + \frac{\varepsilon'_s - \varepsilon'_\infty}{1 + j\omega\tau} - j\frac{\sigma}{\varepsilon_0\omega} \quad (21)$$

Here ε'_s and ε'_∞ are the limiting values of permittivity, and σ the conductivity of the system; ε'_s, ε'_∞ and σ are functions of the permittivities, ε, conductivities, σ, and volume fractions, v, of the constituents and are

given by

$$\varepsilon'_s = \frac{\sum_i \upsilon_i \varepsilon_i / \sigma_i^2}{(\sum_i \upsilon_i / \sigma_i)^2} \tag{22a}$$

$$\varepsilon'_\infty = \frac{1}{\sum_i \upsilon_i / \varepsilon_i} \tag{22b}$$

$$\sigma = \frac{1}{\sum_i \upsilon_i / \sigma_i} \tag{22c}$$

In terms of M' and M'', Equations 21 describing interfacial polarization can also be transformed

$$M' = M_\infty M_s \frac{M_\infty + M_s \omega^2 \tau^2}{M_\infty^2 + M_s^2 \omega^2 \tau^2 + 2M_\infty M_s (M_\infty - M_s)(\sigma\tau/\varepsilon_0) + M_\infty^2 M_s^2 (\sigma/\varepsilon_0 \omega)^2 (1 + \omega^2 \tau^2)} \tag{23}$$

$$M'' = M_\infty M_s \frac{(M_\infty - M_s)\omega\tau + M_\infty M_s (\sigma/\varepsilon_0 \omega)(1 + \omega^2 \tau^2)}{M_\infty^2 + M_s^2 \omega^2 \tau^2 + 2M_\infty M_s (M_\infty - M_s)(\sigma\tau/\varepsilon_0) + M_\infty^2 M_s^2 (\sigma/\varepsilon_0 \omega)^2 (1 + \omega^2 \tau^2)} \tag{24}$$

where

$$M_s = \frac{(\sum_i \upsilon_i / \sigma_i)^2}{\sum_i \upsilon_i \varepsilon_i / \sigma_i^2} \tag{25a}$$

$$M_\infty = \sum_i \upsilon_i / \varepsilon_i \tag{25b}$$

$$\sigma = \sum_i \upsilon_i / \sigma_i \tag{25c}$$

Equations 23 and 24 when $\sigma \to 0$ give the Debye Equations 8 and 9 for a single relaxation time.

Relaxation peaks shown in Figs 2c, 3c, and 4a are attributed to an interfacial polarization process. In the range of frequencies where these peaks are formed only interfacial relaxation processes have been reported for the epoxy resin [24] and no relaxation of any kind for the Kevlar fibres [25]. Further support to this statement is given by Fig. 6. It shows Cole–Cole plots for three different specimens: (a) a composite with 25 p.h.r. Al and 1.5 p.h.r. Kevlar in epoxy resin, (b) a composite with 25 p.h.r. Al in epoxy resin, and (c) a composite with 1.5 p.h.r. Kevlar in epoxy resin. Specimen (a) with higher heterogeneity corresponds to greater dielectric losses and its semicircle is more completely formed compared to specimens (b) and (c). At the same time, the increase in heterogeneity shifts the whole relaxation process to lower frequencies indicating also the MWS nature of the effect.

To distinguish which one of the equations developed describes better the process of interfacial relaxation in these systems, the Cole–Cole plots in electric modulus are again examined. Fig. 7 shows that the Davidson–Cole approach with $\gamma = 0.680$ is best fitted to experimental points of Fig. 5a and the Havriliak–Negami approach with $\gamma = 0.865$ and $\alpha = 0.105$ is best fitted to the experimental points of Fig. 5b. These last values suggest a behaviour close to the state of a single relaxation time. In Fig. 6, experimental points resulting from the composite (c) are best fitted to a curve close to a semicircle with the Davidson–Cole approach and $\gamma = 0.675$. Experimental points resulting from composite (b) of Fig. 6 are best fitted to a semicircle with the Cole–Cole approach and exponent $\alpha = 0.160$. In a previous work [26] concerning composite polymeric systems with epoxy resin and metal powders (copper, iron) interfacial relaxation was better described by the Cole–Cole Equations (11, 12, 13) with $\alpha = 0.156$.

In Fig. 8, two Cole–Cole plots, for different epoxy resin–Kevlar fibre systems are presented. The experimental data of the system with low Kevlar fibre content are best fitted to the Davidson–Cole treatment with exponent $\gamma = 0.805$. In the system, with increased Kevlar content, the same approach leads to a value of $\gamma = 0.670$. Apparently the inclusion of asymmetric particles in composites, such as Kevlar fibres, created an additional asymmetric distribution of relaxation times. It is then concluded that the inclusions intervene in the process of interfacial relaxation. Examining systems with increased heterogeneity, as the hybrid composites of Fig. 9, the same qualitative conclusions are reported. An increase in the Kevlar content results

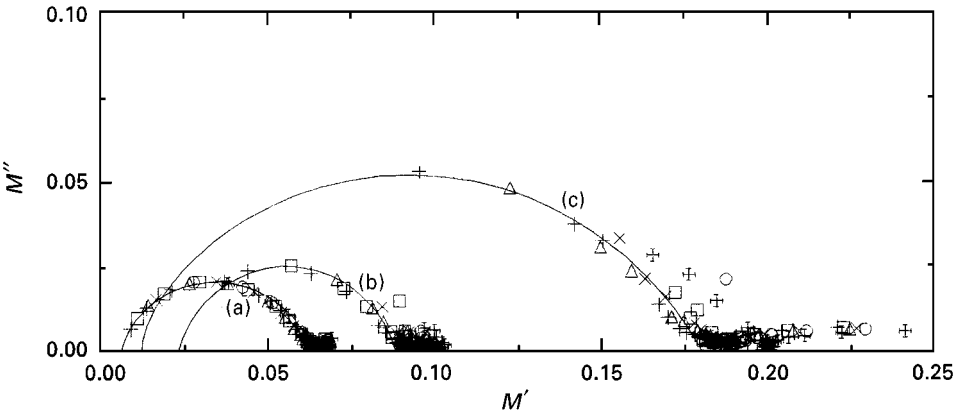

Figure 6 Cole–Cole plots of the systems with (a) 25 p.h.r. in Al and 1.5 p.h.r. in Kevlar fibres. (b) 25 p.h.r. in Al, (c) 1.5 p.h.r. in Kevlar fibres. For key, see Fig. 5.

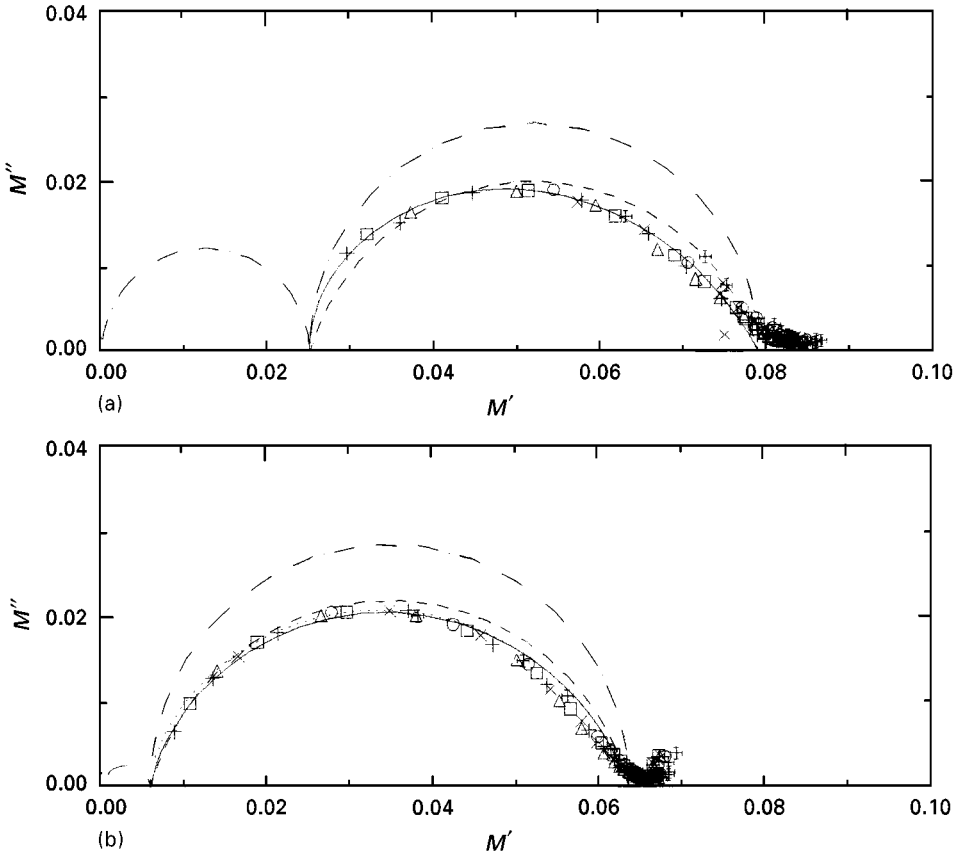

Figure 7 Cole–Cole plots of the systems with 25 p.h.r. in Al and (a) 0.5 p.h.r. (b) 1.5 p.h.r. in Kevlar fibres. Each line represents a different approach: (a) (—·—) MWS approach; (— —) Cole–Cole behaviour with $\alpha = 0.185$. (——) Davidson–Cole approach with $\gamma = 0.680$, which is the best fitted curve to experimental points. (b) (–·–) MWS approach; (- - -) Cole–Cole behaviour with $\alpha = 0.165$; (· · ·) Davidson–Cole behaviour with $\gamma = 0.770$. (—) Havriliak–Negami approach with $\alpha = 0.105$ and $\gamma = 0.865$, which is the best fitted curve to experimental points. For key, see Fig. 5.

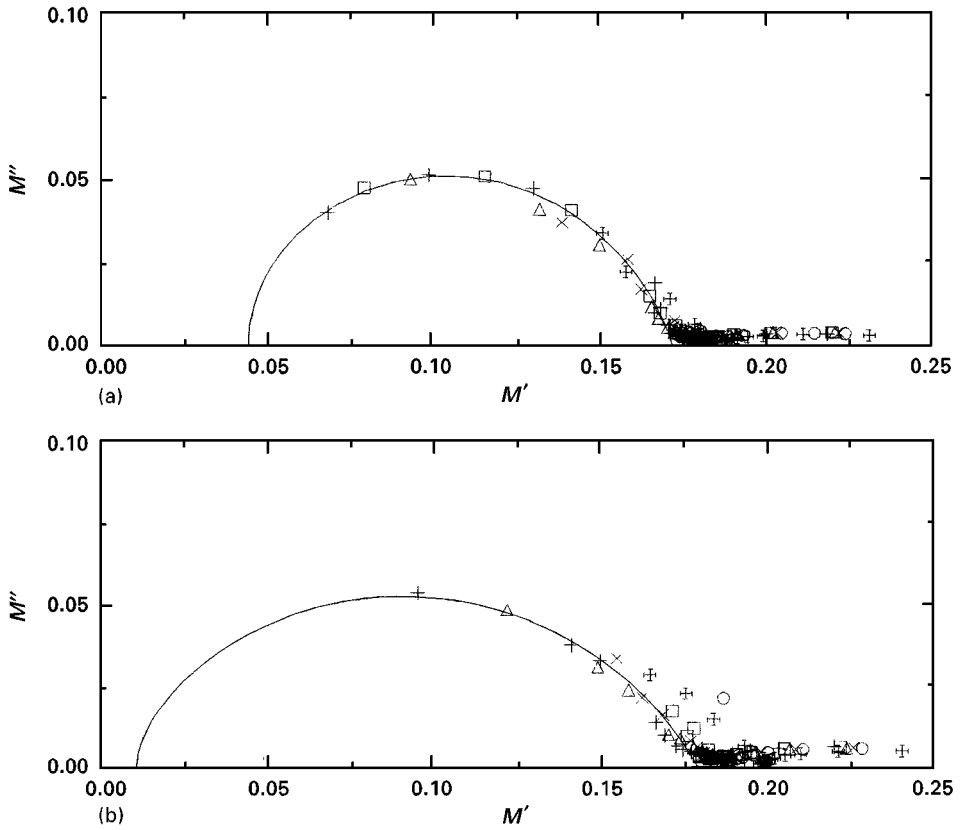

Figure 8 Cole–Cole plots of the systems with (a) 0.5 p.h.r. and (b) 1.5 p.h.r. in Kevlar fibres. Experimental points are best fitted to the Davidson–Cole approach with values of the γ parameter (a) 0.800 and (b) 0.675. For key, see Fig. 5.

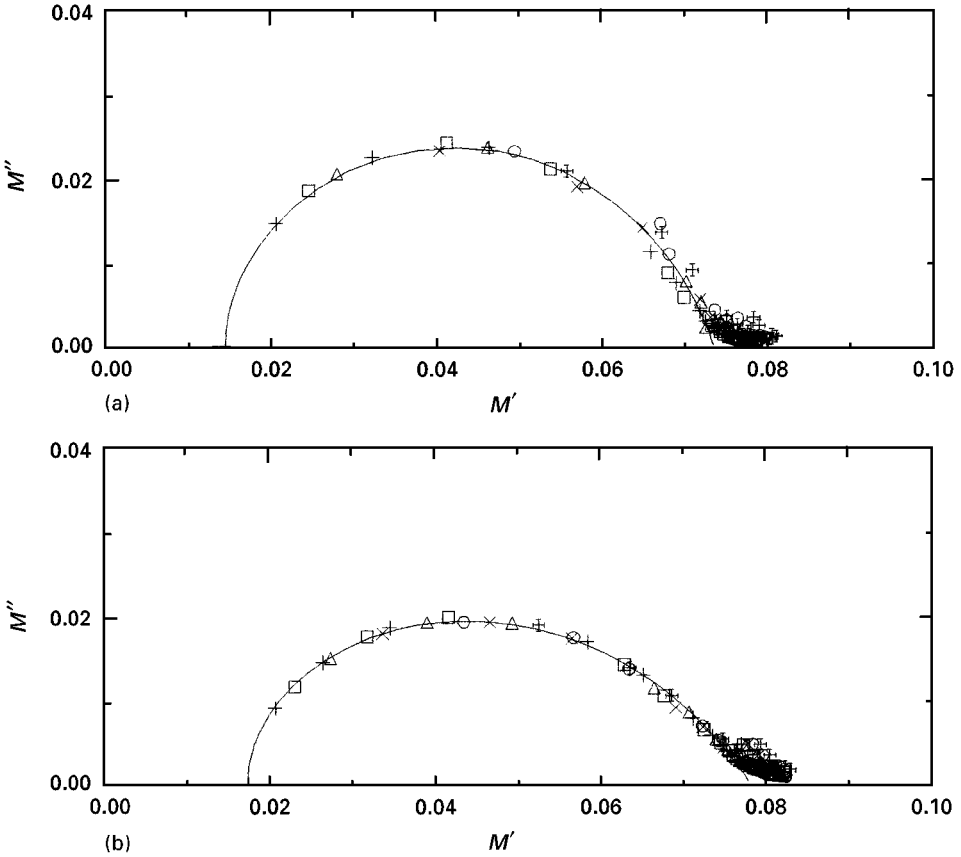

Figure 9 Cole–Cole plots of the hybrid systems with 15 p.h.r. in Al and (a) 0.5 p.h.r., (b) 1.5 p.h.r. in Kevlar fibres. Experimental points are best fitted to the Davidson–Cole approach with values of the γ parameter (a) 0.805 and (b) 0.635. For key, see Fig. 5.

TABLE I Parameters used/evaluated for the Davidson–Cole, Cole–Cole and Havriliak–Negami functions

Composite material	Function	M_s	M_∞	α	γ
Ep. + 0.5 p.h.r. Kevlar	Davidson–Cole	0.0450	0.1720	–	0.800
Ep. + 1.5 p.h.r. Kevlar	Davidson–Cole	0.0120	0.1800	–	0.675
Ep. + 25 p.h.r. Al	Cole–Cole	0.0230	0.0880	0.160	–
Ep. + 15 p.h.r. Al + 0.5 p.h.r. Kevlar	Davidson–Cole	0.0145	0.0735	–	0.805
Ep. + 15 p.h.r. Al + 1.5 p.h.r. Kevlar	Davidson–Cole	0.0170	0.0775	–	0.635
Ep. + 25 p.h.r. Al + 0.5 p.h.r. Kevlar	Davidson–Cole	0.0250	0.0790	–	0.680
Ep. + 25 p.h.r. Al + 1.5 p.h.r. Kevlar	Havriliak–Negami	0.0058	0.0634	0.105	0.865

in a broader asymmetric distribution of relaxation times, the values of parameter γ change from 0.800 to 0.680 for the same change of Kevlar fibre content, as in the previous binary systems. However, examining systems with higher heterogeneity, Fig. 7, this systematic change in the exponent γ, does not appear. In contrast, alteration of Kevlar fibre content from 0.5 p.h.r. to 1.5 p.h.r. and for the same (25 p.h.r.) aluminium powder content produces a narrower distribution of relaxation times, attributed to the intensity of the interfacial polarization effect and to the induced macroscopic homogeneity performance of the materials. All fitting parameters are shown in Table I.

At the low-frequency end, the formed semicircle (Figs 5 and 7) does not reach the origin but has a small positive intersect on the M' axis, evidence of a dielectric relaxation process or of existing electrode polarization [27]. The care taken to achieve good electrical contact between electrodes and specimens and the formation of a semi-circle corresponding to conductivity relaxation, Fig. 7, besides the Maxwell–Wagner–Sillars relaxation process, when using Equations 23–25 and the measured value for conductivity ($\sigma = 1.1 \times 10^{-14}$ ohm^{-1} cm^{-1}), are supporting the first of the two assumptions. At the high-frequency end (Figs 5–7), another process starts which has been attributed to the orientation of dipolar groups [24, 28, 29]. The semicircle at the high-frequency end is a little skewed, and this deviation has also been observed in polystyrene–glass beads composites [30]. It is most probable that this behaviour is connected with the start of a new process as already stated but it also expresses the asymmetrical character of the distribution of relaxation times.

Because, as a result from the above discussion, the Davidson–Cole approach is most suitable for the

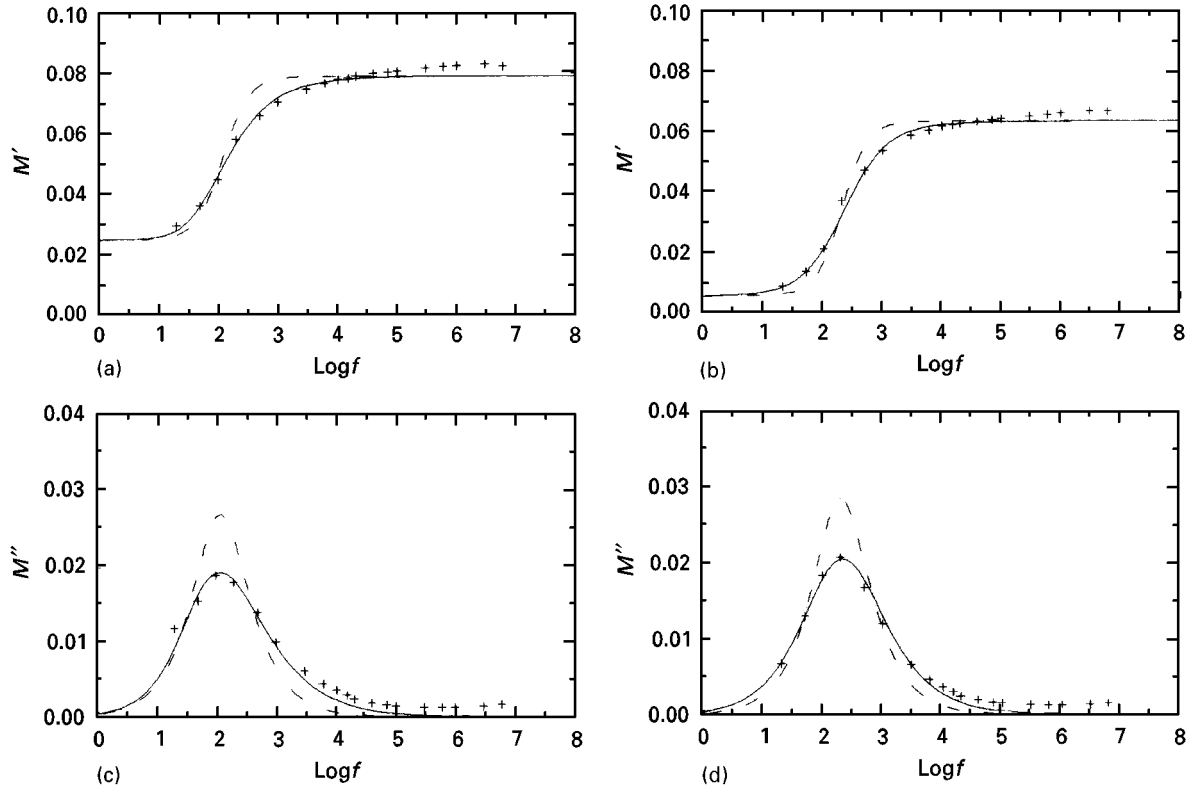

Figure 10 The real part, M' and the imaginary part, M'', of electric modulus, M^* versus frequency, at 150 °C of the composites with 25 p.h.r. in Al and (a, c) 0.5 p.h.r. in Kevlar fibres (b, d) 1.5 p.h.r. in Kevlar fibres. (—) The Davidson–Cole approach in plots (a) and (c) and the Havriliak–Negami approach in plots (b) and (d) (–·–) The MWS approach. (+) Experimental points.

description of interfacial relaxation in the composites with moderate heterogeneity and the Havriliak–Negami approach for the systems with higher heterogeneity, Equations 16, 17 and 19, 20 are represented in Fig. 10a–d together with experimental points at 150 °C. The Maxwell–Wagner–Sillars approach (Equations 23 and 24) is also shown. It can be clearly seen, especially from Fig. 10c and d that the Davidson–Cole and Havriliak–Negami equations fit better to the experimental points. The deviation of the MWS approach from the observed behaviour must be attributed to the presence of a distribution of relaxation times and to the small value of conductivity, σ, of the systems, because as has been noted, for very small values of conductivity the MWS Equations 23 and 24 reduce to those for a pure Debye-like relaxation process (Equations 8 and 9).

The increase in the values of M' and the subsequent development of M'' peaks with increasing frequency is a characteristic behaviour of a dielectric dispersion. The constant value of M' at higher frequencies is due to the fact that interfacial polarization is ineffective at higher frequencies, as large dipoles developed at the interfaces cannot follow the electric field when the frequency is high (Figs 2a, c, 3a, c 10). The small decrease of M' values with the temperature increase in the low-frequency range (Figs 2a, 3a) results from the increased motion of large parts of molecular chains in the polymer as $T_g(\sim 180\,^\circ\text{C})$ is approached. Orientation of the large dipoles at the interfaces becomes easier and permittivity is increased with the consequent decrease in M' values. At higher frequencies, orientation is not possible and temperature becomes

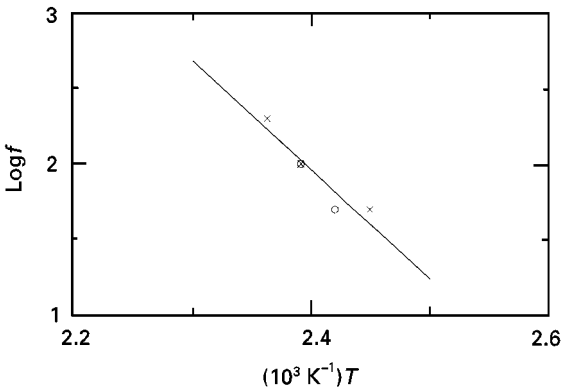

Figure 11 Arrhenius plot of the loss peaks locations versus $1/T$. Data for composites with 0.5 or 1.5 p.h.r. in Kevlar fibres and 25 p.h.r. in Al are scattered about a curve representing the function, $\ln f = A + B/T$ to which data are fitted. The correlation factor is $R = 0.97$.

ineffective. As a consequence of the described behaviour, peaks in the values of M'' (Figs 2c, 3c) are slightly displaced to greater values of frequency.

The decrease in the values of M' with increase in the Kevlar fibre content, as observed in Figs 2a and 3a, is exactly a result of the logarithmic law of mixtures [31], as has also been observed with composites of epoxy resins and Kevlar fibres [32]. Increase in the peak values of M'' is attributed to the increased heterogeneity introduced by the higher content in Kevlar fibres and the consequent increase of the dielectric losses.

The shift in the Cole–Cole plots (Fig. 5) towards the origin with increasing Kevlar fibre content is

understood after the explanation of the change of M' and M'' with change in the fibres content of the composite, thus implying an increase in relaxation time with heterogeneity [18].

Fig. 11 shows the Arrhenius plot of the loss peak locations versus $1/T$. Data for composites with 0.5 or 1.5 p.h.r. in Kevlar fibres and 25 p.h.r. in aluminium are scattered about the same line. An activation energy of 139 kJ mol^{-1} (1.44 eV) is obtained for this MWS relaxation process. A value of 0.87 eV has been reported for a composite with Kevlar fibres and glass beads [33].

As is assumed by the above analysis of the behaviour of the composites examined in this work, the complex permittivity and the complex electric modulus contain the same information. However, it is more effective sometimes to present this information in the electric modulus formalism than in the dielectric mode. The use of imaginary part, M'', over the loss factor, ε'', offers advantages especially in cases where the values of ε'' show a considerable increase (high temperature–low frequency) . The maximum in M'' appears at lower temperatures (or higher frequencies) than the corresponding value of the loss factor ε''. This behaviour implies a decrease in the relaxation time, in the modulus mode, in comparison to the relaxation time in the permittivity mode and this experimental result is in accordance with the theoretical considerations stated earlier. Therefore, using the electric modulus formalism, the peak losses appear at higher frequencies offering a significant advantage, especially in the case of relaxation in the low-frequency region like MWS, also making possible the determination of activation energy of the process. Furthermore, the presence of ε' in the denominator to the second power in the function giving M'' (Equation 1) minimizes the tendency of ε', because of its high values, to overwhelm the loss function ($\mathrm{tg}\,\delta = \varepsilon''/\varepsilon' = M''/M'$).

Finally, the contribution of electrode polarization effects on the M' data can be very small, if care has been taken to ensure good ohmic contact between the electrodes and the sample, as in the case of the silver paint contacts. Thus, the necessity for any correction of the M' values is actually becoming negligible and the data obtained in the electric modulus mode can be treated accordingly [10, 13, 34].

5. Conclusion

The formalism of electric modulus is considered suitable for the investigation of the dielectric behaviour of polymeric composites with a conductive component. It is capable of revealing interfacial relaxation which, in most cases, is covered by the conductivity of the material.

All equations describing relaxations in the dielectric terminology, e.g. Debye, Cole–Cole, Davidson–Cole, Havriliak–Negami, and Sillars, are transformed and expressed in the electric modulus mode.

In the binary composites of epoxy resin with Kevlar fibres and in hybrid composites of epoxy resin with Kevlar fibres and aluminium particles as fillers, interfacial polarization is best described by the Davidson–Cole approach because of the asymmetric distribution of relaxation times due to the presence of particles in the composites. In hybrid composites with greater filler content and thus higher heterogeneity, the interfacial relaxation process is best described by the Havriliak–Negami approach with values of α and γ parameters corresponding to a narrow distribution of relaxation times. This behaviour can be considered to respond to an induced macroscopic homogeneity performance of the systems as a result of the increased value of filler content.

References

1. J. C. MAXWELL, "Electricity and Magnetism" Vol. 1 (Clarendon, Oxford, 1892) p. 452.
2. K. W. WAGNER, *Arch. Electrotech.* **2** (1914) 371.
3. R. W. SILLARS, *J. Inst. Elect. Eng.* **80** (1937) 378.
4. B. K. P. SCAIFE, "Principles of Dielectrics" (Clarendon, Oxford, 1989), p. 291.
5. L. K. H. van BECK, in "Progress in Dielectrics", Vol. 7, edited by J. B. Birks, Heywood Books, Cleveland, OH, 1967) p. 69.
6. A. R. von HIPPEL, "Dielectrics and Waves" (Wiley, New York, 1954) p. 228.
7. C. J. F. BÖETTCHER and P. BORDEWIJK, "Theory of Electric Polarization" Vol II (Elsevier, Amsterdam, 1978) p. 486.
8. P. HEDVIG, "Dielectric Spectroscopy of Polymers" (Adam Hilger, Bristol, 1977) p. 293.
9. N. G. McCRUM, B. E. READ and G. WILLIAMS, "Anelastic and Dielectric Effects in Polymeric Solids" (Wiley, London, 1967) pp. 108–111.
10. P. B. MACEDO, C. T. MOYNIHAN and R. BOSE, *Phys. Chem. Glasses* **13** (1972) 171.
11. A. A. BAKR and A. M. NORTH, *Eur. Polym. Sci.* **13** (1977) 799.
12. H. W. STARKWEATHER and P. AVAKIAN, *J. Polym. Sci. B Polym. Phys.* **30** (1992) 637.
13. SHOW-AN CHEN and CHIEN-SHIUN LIAO, *Macromolecules* **26** (1993) 2810.
14. I. M. HODGE and A. EISENBERG, *J. Non-Cryst. Solids* **27** (1978) 441.
15. F. S. HOWELL, R. A. BOSE, P. B. MACEDO and C. T. MOYNIHAN, *J. Phys. Chem.* **78** (1974) 639.
16. R. P. SHELDOM, "Composite Polymeric Materials" (Applied Science, London, 1982) p. 74.
17. E. I. DU PONT DE NEMOURS & Co. (Inc.), Product data sheet, 1986.
18. G. M. TSANGARIS, G. C. PSARRAS and A. J. KONTOPOULOS, *J. Non-Cryst. Solids* **131-133** (1991) 1164.
19. K. S. COLE and R. H. COLE, *J. Chem. Phys.* **9** (1941) 341.
20. C. J. F. BÖETTCHER and P. BORDEWIJK, "Theory of Electric Polarization", Vol. II (Elsevier, Amsterdam, 1978) p. 62.
21. R. H. BOYD, in "Electrical Methods in Methods of Experimental Physics", Vol. 16, part C, "Polymers-Physical Properties", edited by R. A. Fava (Academic Press, New York, 1980) p. 390.
22. D. W. DAVIDSON and R. H. COLE, *J. Chem. Phys.* **18** (1950) 1417.
23. S. HAVRILIAK and S. NEGAMI, *J. Polym. Sci. C* **14** (1966) 99.
24. V. BAZIARD, S. BRETON, S. TOUTAIN and A. GOURDENNE, *Eur. Polym. J.* **24** (1988), 521.
25. "ASM Engineering Materials Handbook", Vol. I, "Composites" (ASM International, Cleveland, OH, 1987), p. 361
26. G. M. TSANGARIS, N. KOULOUMBI and S. KYVELIDIS, *J. Mater. Chem. Phys.* **44** (1996) 245.
27. D. R. DAY, Y. J. LEWIS, H. L. LEE and S. D. SENTURIA, *J. Adhesion* **18** (1985) 73.
28. Y. BAZIARD, S. BRETON, S. TOUTAIN and A. GOURDENNE, *Eur. Polym. J.* **24** (1988) 633.

29. P. HEDVIG, "Dielectric Spectroscopy of Polymers" (Adam Hilger, Bristol, 1977) p. 285.
30. G. PERRIER and A. BERGERET, *J. Appl. Phys.* **77** (1995) 2651.
31. K. LICHTENECKER and K. RÖTHER, *Phys. Z.* **32** (1931) 255.
32. G. M. TSANGARIS and G. C. PSARRAS, *Adv. Compos. Lett.* **4** (1995) 125.
33. P. D. ALDRICH, R. L. McGEE, S. YALVAC, J. E. BONEKAMP and S. W. THUOW, *J. Appl. Phys.* **62** (1987) 4504.
34. A.S. NOWICK and B. S. LIM, *J. Non-Cryst. Solids* **172-174** (1994) 1389.

Received 4 February
and accepted 5 December 1997